

Two-dimensional heterostructures based on ZnO

A.A. Lotin · O.A. Novodvorsky · L.S. Parshina ·
E.V. Khaydukov · D.A. Zuev · O.D. Khramova ·
V.Y. Panchenko

Received: 23 October 2010 / Revised version: 18 March 2011 / Published online: 30 April 2011
© Springer-Verlag 2011

Abstract The multiple quantum wells (MQW) $\text{Mg}_{0.27}\text{Zn}_{0.73}\text{O}/\text{ZnO}$ have been grown by the pulsed laser deposition method with different well widths L_w . The interface roughness of quantum wells was inherited from the bottom one and did not exceed 1 nm. We observed the quantum confinement effect showing up in the blue shift of the exciton peak in the low temperature (8 K) photoluminescence and absorption spectra at well width reduction. The exciton binding energy of the two-dimensional structures $\text{Mg}_{0.27}\text{Zn}_{0.73}\text{O}/\text{ZnO}$ was two times higher in comparison with the bulk ZnO. It has been established that Einstein's characteristic temperature Θ_E sharp increase with reduction of well width L_w up to $L_w = 2.6$ nm. It has been revealed that the discontinuity ratio of conduction and valence bands in the heterostructure $\text{Mg}_{0.27}\text{Zn}_{0.73}\text{O}/\text{ZnO}$ is 0.65/0.35. We demonstrated the abrupt increase in quantum efficiency at a reduction of the well width that allowed us to observe the optically excited stimulated emission in ZnO quantum wells with the excitation threshold of ~ 210 kW/cm².

1 Introduction

Semiconductor two-dimensional structures, such as quantum wells (QW) and superlattices, serve for more than decades as a basis for a wide spectrum of optoelectronic devices. Recently, great attention has been given to wide

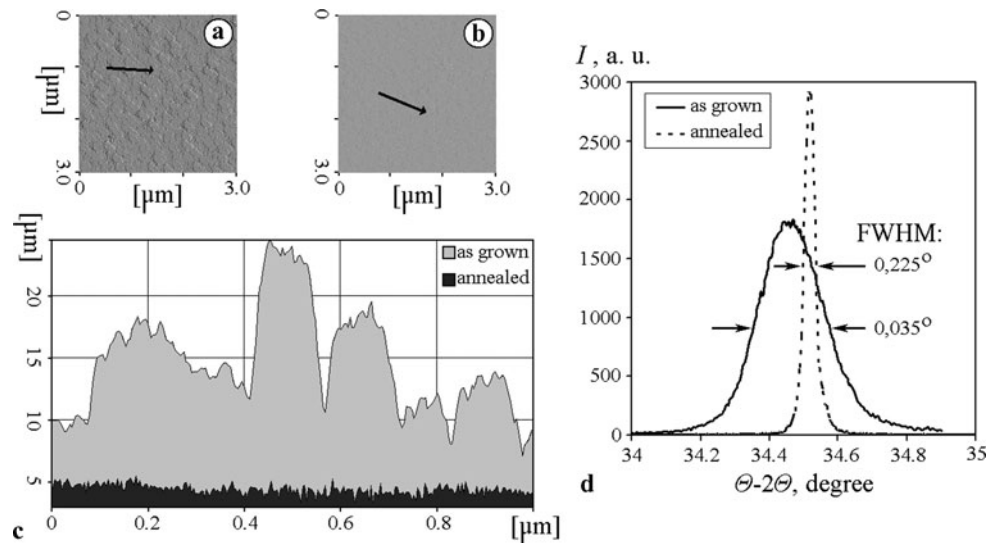
gap semiconductors because optoelectronic devices based on the capability of working in ultraviolet and visible spectral ranges [1–3]. Of particular interest is zinc oxide, thanks to the wide band gap $E_g = 3.37$ eV and high exciton binding energy 60 meV that provides effective exciton emission at higher temperatures in comparison with III–V optical semiconductors [4]. High heat conductivity, effective luminescence, mechanical, and chemical resistance allow the devices based on ZnO to work under extreme conditions. The control of the semiconductor band gap is one of the major problems of optoelectronics. The ternary composition $\text{Mg}_x\text{Zn}_{1-x}\text{O}$ can be used as a heteropair for ZnO and as a barrier in corresponding QW. Increasing of x leads to the blue shift of the band gap.

The excitons in the quantum wells based on ZnO have a higher stability in comparison with III–V QW because of an exciton binding energy increase and exciton-phonon interaction reduction, caused by quantum confinement. Thanks to these effects, the excitons are expected to play an important role in such processes as stimulated radiation in the multiple quantum wells based on zinc oxide even at room temperature [5].

In the present work, a series of $\text{Mg}_{0.27}\text{Zn}_{0.73}\text{O}/\text{ZnO}$ MQWs with different well widths has been grown. The quantum confinement effect showing up in the blue shift of the exciton peak and the increasing exciton peak intensity in photoluminescence spectra (PL), the exciton binding energy, and Einstein's characteristic temperature have been investigated under well width reduction. The values of conductivity and valence bands discontinuity in the heterostructure $\text{Mg}_{0.27}\text{Zn}_{0.73}\text{O}/\text{ZnO}$ have been defined. The structural properties of $\text{Mg}_{0.27}\text{Zn}_{0.73}\text{O}/\text{ZnO}$ have been investigated. The optical amplification in the two-dimensional heterostructures based on ZnO has been demonstrated.

A.A. Lotin (✉) · O.A. Novodvorsky · L.S. Parshina ·
E.V. Khaydukov · D.A. Zuev · O.D. Khramova · V.Y. Panchenko
Institute on Laser and Information Technologies, Russian
Academy of Sciences (ILIT RAS), 1 Svyatoozerskaya St., 140700
Shatura, Moscow Region, Russia
e-mail: Lotin_82@mail.ru
Fax: +7-49645-22532

Fig. 1 The surface morphology of the buffer layer $\text{Mg}_{0.27}\text{Zn}_{0.73}\text{O}$ on a *c*-sapphire substrate (00.1): (a) as grown, (b) annealed at 1000°C, (c) cross-section profiles of corresponding surfaces, (d) the θ - 2θ scans of the $\text{Mg}_{0.27}\text{Zn}_{0.73}\text{O}$ thin buffer layer as-grown (solid line) and annealed at 1000°C (dashed line)



2 Experimental details

The series of multiple quantum wells $\text{Mg}_{0.27}\text{Zn}_{0.73}\text{O}/\text{ZnO}$ with the well width ranging from 1 nm to 20 nm was grown on *c*-sapphire substrates (00.1) by the pulsed laser deposition method. The growth of MQW was carried out in a high vacuum chamber with initial vacuum below 10^{-7} Torr. The ablation of ceramic targets was performed by the excimer laser LC-7020 at a pulse repetition frequency of 10 Hz ($\lambda = 248$ nm, $\tau = 15$ ns; the energy density of laser radiation on the target was 4 J/cm^2). The details of experimental setup have already been reported in [6].

As the mismatch of the lattice parameter a between the ZnO lattices and the *c*-sapphire (00.1) substrate is $\sim 18\%$, the buffer layer $\text{Mg}_{0.27}\text{Zn}_{0.73}\text{O}$ of ~ 100 nm thickness was preliminarily grown on the substrate. The thickness b of individual barrier layers $\text{Mg}_{0.27}\text{Zn}_{0.73}\text{O}$ and the total thickness m^*L_w of ZnO layers was constant for all the MQW ($b = 6$ nm and $m^*L_w = 50$ nm, m —the number of periods). The substrate temperature during the growth was maintained in the range of $(450 \pm 5)^\circ\text{C}$. The substrates were mounted within 7 cm from the targets. For achievement of an atomic-smooth surface, the substrates with the first grown buffer layer $\text{Mg}_{0.27}\text{Zn}_{0.73}\text{O}$ were annealed for 2 hours in the oxygen atmosphere at the temperature of 1000°C. Oxygen (O_2) was used as a buffer gas; its pressure in the chamber was 5 mTorr.

To study the optical properties of the MQW, the low temperature (8 K) spectra of photoluminescence and absorption were measured in the short-wave range. The PL excitation was carried out by a continuous-wave He–Cd laser ($\lambda = 325$ nm, $W = 20$ mW) and a pulsed-periodical KrF excimer laser. The PL spectra were registered by a HR4000 spectrometer (Ocean Optics) and the absorption spectra were recorded by a Cary-50 spectrophotometer (Var-

ian). The investigation of structural characteristics, diffusion processes, and interface quality of the multiple quantum wells $\text{Mg}_{0.27}\text{Zn}_{0.73}\text{O}/\text{ZnO}$ was performed by the multipurpose X-ray diffractometer D8 Discover (Bruker-AXS). The surface morphology was investigated by the atomic force microscope (AFM) DME DualScope 2401.

3 Results and discussion

3.1 Buffer layer preparation for ZnO quantum wells

The surface morphology of the buffer layer $\text{Mg}_{0.27}\text{Zn}_{0.73}\text{O}$ determined by the atomic force microscopy method has shown that the surface roughness after the deposition is 5–15 nm. To reduce the surface roughness, the substrates with buffer layers were subjected to thermal annealing at the temperature of 1000°C in oxygen atmosphere. From Fig. 1b, c, it is seen that the roughness of the surface after this treatment did not exceed 1 nanometer.

The results of X-ray diffraction showed that the full width on a half maximum (FWHM) of the peak near (00.2) unit of the as-grown buffer layer $\text{Mg}_{0.27}\text{Zn}_{0.73}\text{O}$ is 0.225° (Fig. 1d). High temperature annealing of the buffer layer $\text{Mg}_{0.27}\text{Zn}_{0.73}\text{O}$ leads to a reduction of FWHM down to 0.035° . Smoothing of the surface and X-ray peak FWHM decrease are associated with reduction of defects and improvement in crystallinity of the thin film due to the high temperature annealing.

3.2 Structural properties of ZnO quantum wells

The structural properties of the two-dimensional heterostructures $\text{Mg}_{0.27}\text{Zn}_{0.73}\text{O}/\text{ZnO}$ were examined by X-ray diffraction and by the reflectometry method. The X-ray analysis of the ZnO and $\text{Mg}_{0.27}\text{Zn}_{0.73}\text{O}$ films indicated that their

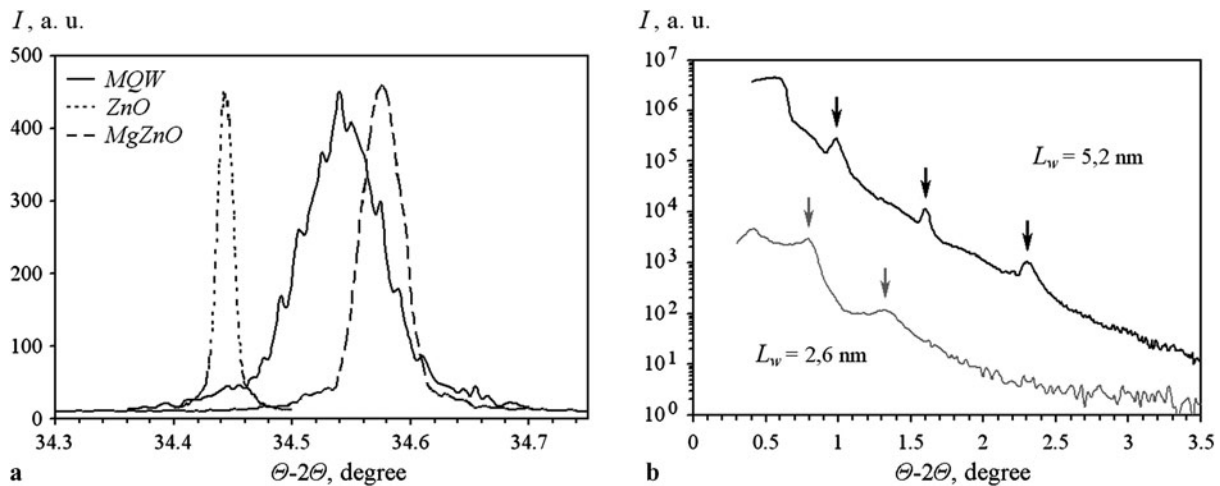


Fig. 2 Normalized θ - 2θ scans of ZnO, the $\text{Mg}_{0.27}\text{Zn}_{0.73}\text{O}$ films and the MQW $\text{Mg}_{0.27}\text{Zn}_{0.73}\text{O}/\text{ZnO}$ with the well width $L_w = 2.6$ nm (a). A curve of mirror reflection of the MQW $\text{Mg}_{0.27}\text{Zn}_{0.73}\text{O}/\text{ZnO}$ with the well widths $L_w = 5.2$ nm and $L_w = 2.6$ nm (b)

lattice mismatch was $\Delta a/a = 0.66\%$. In Fig. 2a are shown the normalized θ - 2θ scans of the ZnO, $\text{Mg}_{0.27}\text{Zn}_{0.73}\text{O}$ thin films and the MQW based on them. The characteristic period of signal modulation and the special software package LEPTOS were used to define the width $L_w = 2.6$ nm of a single well that agrees well with the expected thicknesses set by the growth rate. To evaluate the quality of interfaces, the chart of reciprocal space has been measured in the vicinity of point (000) of the reciprocal lattices (a curve of mirror reflection). Figure 2b presents the curve of mirror reflection of the MQW $\text{Mg}_{0.27}\text{Zn}_{0.73}\text{O}/\text{ZnO}$, which has been obtained by subtraction of the diffuse scattering distribution from the experimental θ - 2θ curve. The presence of the resonant diffraction scattering effect indicates to the correlation in interface morphology in the whole structure, i.e., roughnesses of the top layers are inherited from the bottom ones and do not exceed 1 nm.

Figure 3 shows the cross-section image of 10 chipped quantum wells $\text{Mg}_{0.27}\text{Zn}_{0.73}\text{O}/\text{ZnO}$ with the well width $L_w = 20$ nm and the barrier width $b = 18$ nm produced by the scanning electron microscopy (SEM). This MQW was specially grown for SEM imaging.

3.3 Excitons in ZnO quantum wells

Studying of optical properties of 2D systems based on ZnO provides interesting information about the excitons in these systems. Therefore, we carried out investigations of photoluminescence and absorption spectra of the $\text{Mg}_{0.27}\text{Zn}_{0.73}\text{O}/\text{ZnO}$ MQW. The band gap of the buffer and barrier layers of $\text{Mg}_{0.27}\text{Zn}_{0.73}\text{O}$ was 3.82 eV, and for the ZnO well layer it was 3.36 eV [7]. The low temperature photoluminescence and absorption spectra (at 8 K) of the multiple quantum wells $\text{Mg}_{0.27}\text{Zn}_{0.73}\text{O}/\text{ZnO}$ with the well width

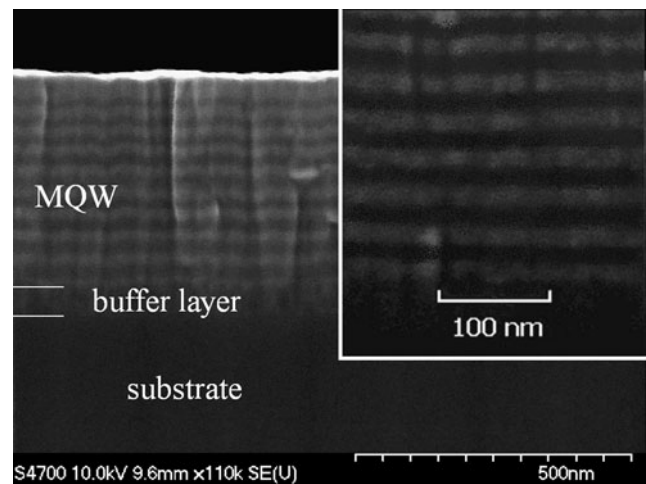
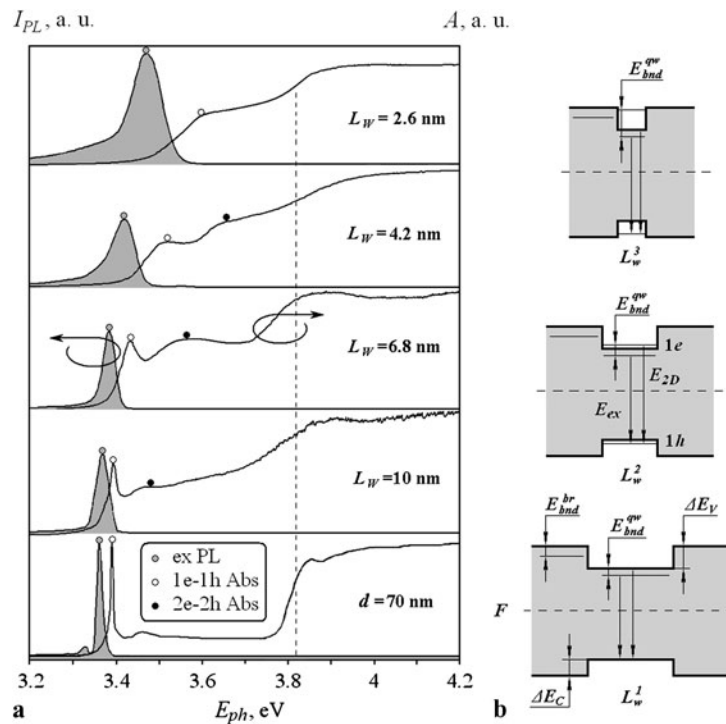


Fig. 3 A SEM-image of cross-section of 10 chipped quantum wells $\text{Mg}_{0.27}\text{Zn}_{0.73}\text{O}/\text{ZnO}$ grown on a sapphire substrate (00.1) with a buffer layer $\text{Mg}_{0.27}\text{Zn}_{0.73}\text{O}$

L_w varying from 2.6 nm to 10 nm are presented in Fig. 4a. The PL and absorption spectra of the 70 nm ZnO film are presented in this figure for comparison. The monotonous nonlinear blue shift of the UV exciton peak position E_{ex} in the spectra for reduced quantum well width characterizes the quantum confinement effect in the two-dimensional heterostructures based on ZnO which has been studied by the authors previously [8].

The important parameter in designing heterostructures is the value of energy band discontinuity in the conduction and valence bands. The solution of Schrödinger equation for a finite square potential well under the condition of symmetry and continuity of the wave function in the conduction and

Fig. 4 (a) The low temperature (8 K) photoluminescence and absorption spectra of the MQW $\text{Mg}_{0.27}\text{Zn}_{0.73}\text{O}/\text{ZnO}$ with various well widths L_w and the thin film ZnO ($d = 70$ nm). (b) The energy diagrams of a single QW $\text{Mg}_{0.27}\text{Zn}_{0.73}\text{O}/\text{ZnO}$ demonstrating the enhancement of exciton binding energy in QW: ΔE_C and ΔE_V —the discontinuities in the conduction and valence bands, $E_{\text{bnd}}^{\text{br}}$ and $E_{\text{bnd}}^{\text{qw}}$ —the exciton binding energy of the barrier layer $\text{Mg}_{0.27}\text{Zn}_{0.73}\text{O}$ and the ZnO QW, respectively, F —Fermi level, and $L_w^1 > L_w^2 > L_w^3$. $1e$ and $1h$ —main electron and hole energy levels in QW



valence bands is possible to obtain as follows [9]:

$$\begin{aligned} & \text{tg} \left[\sqrt{\frac{2m_{1(e,h)}^* E_n^{(e,h)}(L_w)}{\hbar^2}} L_w \right] \\ &= \sqrt{\frac{m_{2(e,h)}^* (\Delta E_{C,V}) - E_n^{(e,h)}(L_w)}{m_{1(e,h)}^* E_n^{(e,h)}(L_w)}}, \end{aligned} \quad (1)$$

where \hbar —Planck's constant, E_n^e and E_n^h —the proper values of energy in the potential wells for an electron and a hole, respectively, $n = 1, 2, 3, \dots$ —an integer number, ΔE_C and ΔE_V —the discontinuities in the conduction and valence bands. The values of electron and hole effective masses have been chosen as $m_{1e}^* = 0.28m_0$ and $m_{1h}^* = 0.78m_0$ for the well active layer of ZnO [10, 11] and $m_{2e}^* = 0.4m_0$ and $m_{2h}^* = 2m_0$ for the barrier layers of $\text{Mg}_{0.27}\text{Zn}_{0.73}\text{O}$ [12]. Within the limits of the given model, the light holes were not considered.

The resulting exciton energy in a quantum well in the main state ($n = 1$) will be defined by the expression:

$$E(L_w) = E_g(\text{ZnO}) + E_1^e(L_w) + E_1^h(L_w). \quad (2)$$

Figure 5a illustrates the dependence of energy position of the photoluminescence exciton peak E_{ex} and the absorption peak E_{Abs} (or E_{2D} —the energy of $1e-1h$ transition in the QW case) in a MQW on the well width L_w . The relation between the discontinuities of the conduction band ΔE_C and valence band ΔE_V was used as a fitting parameter. The best

coincidence of the numerical and experimental data has been obtained at the ratio of $\Delta E_C/\Delta E_V = 0.65/0.35$ that is in good agreement with the results found in the literature [11, 13].

The FWHM of the PL exciton peak in the MQW also increased with a reduction of the quantum well width L_w (Fig. 4a) that can be explained by random fluctuation of the width $L_w \pm \delta L_w$ and the barrier height of quantum wells, which leads to nonuniform broadening of the photoluminescence spectrum. The QW barrier height fluctuation is caused by Mg content inhomogeneity in the barriers. The smaller the width of a well L_w , the higher is the influence of this fluctuation δL_w on FWHM of exciton peak in the photoluminescence spectra and the degradation of absorption spectra of MQW [14]. For these reasons, the E_{2D} value of MQW with $L_w = 1$ nm was not possible to define.

The confinement of charge carriers in one of the coordinates leads to an increase of exciton binding energy of a two-dimensional (2D) exciton in the main state in comparison with a three-dimensional (3D) one. This phenomenon is illustrated in Fig. 4b. It is known that exciton energy is described as [15]:

$$E_{\text{ex}} = E_g - E_{\text{bnd}} + E_k, \quad (3)$$

where E_g —the band gap (E_{2D}), E_{bnd} —the exciton binding energy, and the third term E_k —the kinetic energy of exciton. The kinetic energy of exciton tends to zero at the temperature $T = 0$ K, therefore, the exciton binding energy in the quantum well will be defined as the difference between the

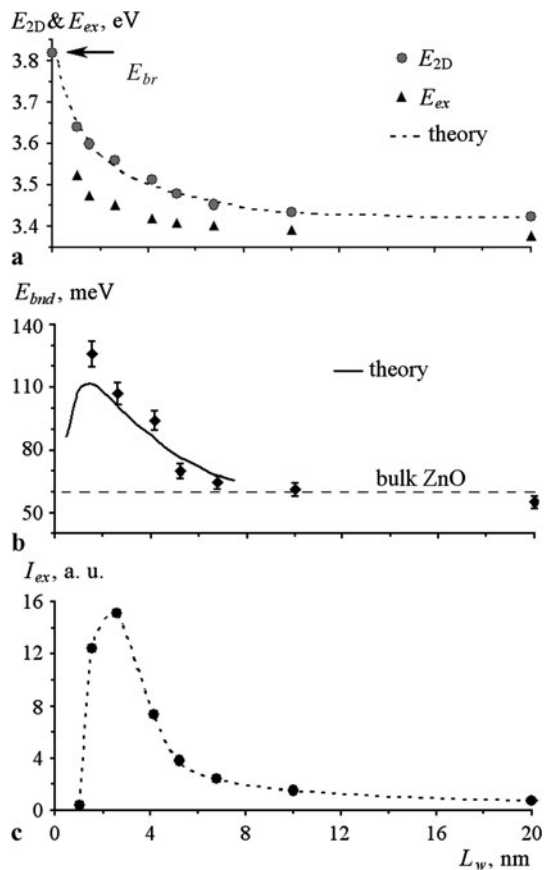


Fig. 5 (a) The dependences of energy position of the photoluminescence exciton peak E_{ex} and the absorption peak E_{2D} in the MQW $\text{Mg}_{0.27}\text{Zn}_{0.73}\text{O}/\text{ZnO}$ on well width L_w (nm). (b) The theoretical [13] and experimental dependences of the exciton binding energy E_{bnd} in the MQW $\text{Mg}_{0.27}\text{Zn}_{0.73}\text{O}/\text{ZnO}$ on quantum well width L_w . (c) The dependence of the MQW $\text{Mg}_{0.27}\text{Zn}_{0.73}\text{O}/\text{ZnO}$ PL intensity on the well width $I_{ex}(L_w)$

energy of $1e-1h$ transition E_{2D} in the absorption spectra and the energy position of exciton peak in the PL spectra E_{ex} :

$$E_{bnd} = E_{2D} - E_{ex}. \quad (4)$$

Figure 5b indicates the dependence of the exciton binding energy E_{bnd} in the MQW $\text{Mg}_{0.27}\text{Zn}_{0.73}\text{O}/\text{ZnO}$ on the quantum well width L_w is achieved by the experimental PL and absorption spectra (Fig. 4) and (4). The theoretical curve $E_{bnd}(L_w)$ for the $\text{Mg}_{0.27}\text{Zn}_{0.73}\text{O}/\text{ZnO}$ 2D system plotted by Coli and Bajaj in [13] is presented here for comparison. The interaction between the charge carriers significantly differs from Coulomb interaction at small distances, due to dielectric inhomogeneity of the periodic 2D structure and charge carrier confinement. This leads to a growth of the binding energy of a two-dimensional exciton under the condition that the exciton radius a_{ex} considerably exceeds the well width L_w in the main state. The maximum value of exciton binding energy obtained by us in the MQW

$\text{Mg}_{0.27}\text{Zn}_{0.73}\text{O}/\text{ZnO}$ (at $L_w = 2.6$ nm) exceeded the value E_{bnd} for the bulk zinc oxide (60 meV) two times.

The nonlinear growth of the exciton peak intensity I_{ex} (Fig. 5c) in the PL spectra was observed for a well width (L_w) reduction in the two-dimensional structures $\text{Mg}_{0.27}\text{Zn}_{0.73}\text{O}/\text{ZnO}$. The maximum value of photoluminescence intensity was observed also at the well width $L_w = 2.6$ nm and was 35 times higher than PL intensity of thin film ZnO; further reduction of L_w causes a sharp decrease in PL intensity. Such behavior of the exciton peak intensity can be explained if it is assumed that the high bulk (3d) concentration of charge carriers can be obtained at well width reduction. The charge carrier life time τ is reduced due to amplification of emission recombination that leads to the growth of quantum efficiency [16]. The abrupt decrease of PL intensity I_{ex} for $L_w < 2.6$ nm can be explained from the quantum well width L_w getting comparable with the value of interface roughness which is ~ 1 nm; excitons undergo scattering on these irregularities, which leads to quenching of photoluminescence.

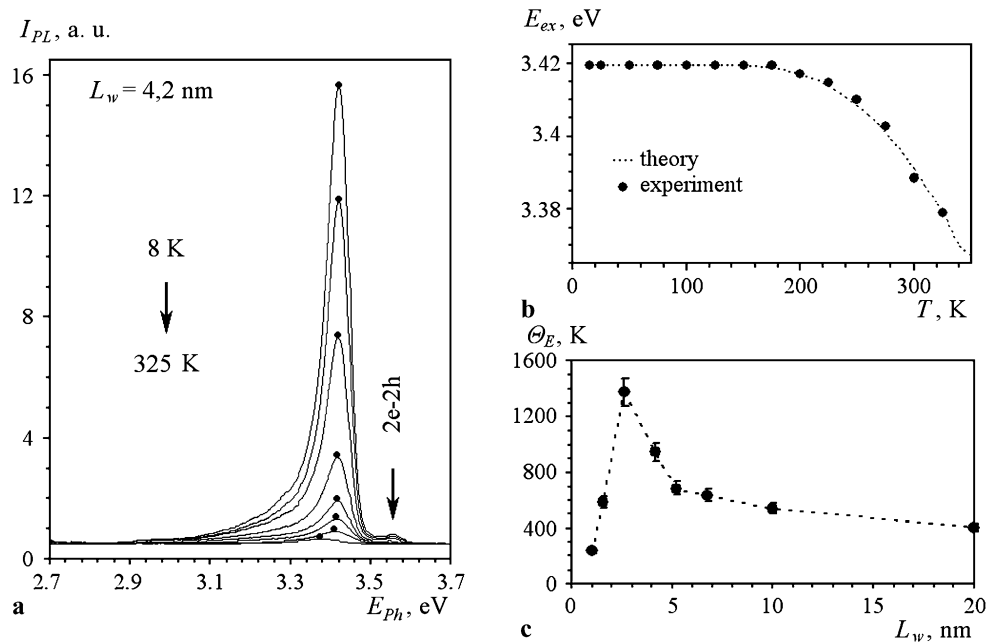
According to the Bose–Einstein model, the exciton energy is expected to vary with the temperature under the following law [17]:

$$E(T) = E(0) - \frac{2\alpha_E}{\exp(\frac{\Theta_E}{T}) - 1}, \quad (5)$$

where α_E —a constant corresponding to exciton-phonon interaction, $\Theta_E = hf/k$ —Einstein’s characteristic temperature, h —Planck’s constant, k —Boltzmann constant, and f —the frequency of phonon fluctuations. Einstein’s characteristic temperature Θ_E —the physical constant of materials characterizing their properties such as a thermal capacity, heat conductivity, the line broadening in X-ray spectra, and others. The materials are described by the laws of quantum physics at temperature T lower Einstein’s characteristic temperature ($T < \Theta_E$), and in the range of high temperature by laws of classical physics. To define the character of Einstein’s temperature Θ_E dependence on quantum well width, we studied the temperature dependence of the photoluminescence spectra of the MQW $\text{Mg}_{0.27}\text{Zn}_{0.73}\text{O}/\text{ZnO}$. The PL spectra of the MQW ($L_w = 4.2$ nm) in a range of temperatures 8–325 K are presented on Fig. 6a, b, and (5) depict the temperature dependence of the exciton energy position E_{ex} , obtained from these spectra. The theoretical dependence (5) derived from the adjustment of α_E and Θ_E parameters is also presented.

Einstein’s characteristic temperature Θ_E was defined for all the two-dimensional heterostructures $\text{Mg}_{0.27}\text{Zn}_{0.73}\text{O}/\text{ZnO}$ by a similar approximation of (5). Figure 6c presents the dependence of Einstein’s characteristic temperature Θ_E on quantum well width L_w . It is seen that Θ_E increases from 410 K up to 1400 K for a reduction of the quantum well

Fig. 6 The PL exciton intensity I_{ex} dynamics (a), the theoretical and experimental dependences of PL exciton energy position (b) of the MQW $Mg_{0.27}Zn_{0.73}O/ZnO$ (6 nm/4.2 nm) on the temperature in the range 8–325 K. The dependence of Einstein's characteristic temperature Θ_E of the MQW $Mg_{0.27}Zn_{0.73}O/ZnO$ on the quantum well width L_w (c)



width in the range from 70 nm to 2.6 nm, and a further decrease of L_w results in a sharp reduction of Θ_E . The growth of Einstein's characteristic temperature Θ_E of ZnO 2D systems means the reduction of exciton–phonon interaction, caused by quantum confinement of charge carriers. Thus, the 2D excitons can exist at much higher temperatures in comparison with 3D ones. The sharp enhancement of quantum efficiency of MQW for a reduction of L_w (Fig. 5c) is also caused by similar reason. The abrupt decrease of Θ_E for $L_w < 2.6$ nm can also be caused by exciton scattering on irregularities.

3.4 Stimulated emission in ZnO quantum wells

As noted above, the excitons are expected to play an important role in stimulated radiation [5]. To study the possibility of stimulated radiation in MQW, the photoluminescence spectra have been investigated with respect to the power density of the excitation radiation applied with an excimer KrF laser at room temperature. Figure 7a presents the photoluminescence spectra of the MQW $Mg_{0.27}Zn_{0.73}O/ZnO$ with the well width $L_w = 5.2$ nm, measured at the room temperature when pumping with an excimer KrF laser at an intensity up to 400 kW/cm². For comparison, the PL spectrum of the same structure excited by a continuous He–Cd laser is also shown here.

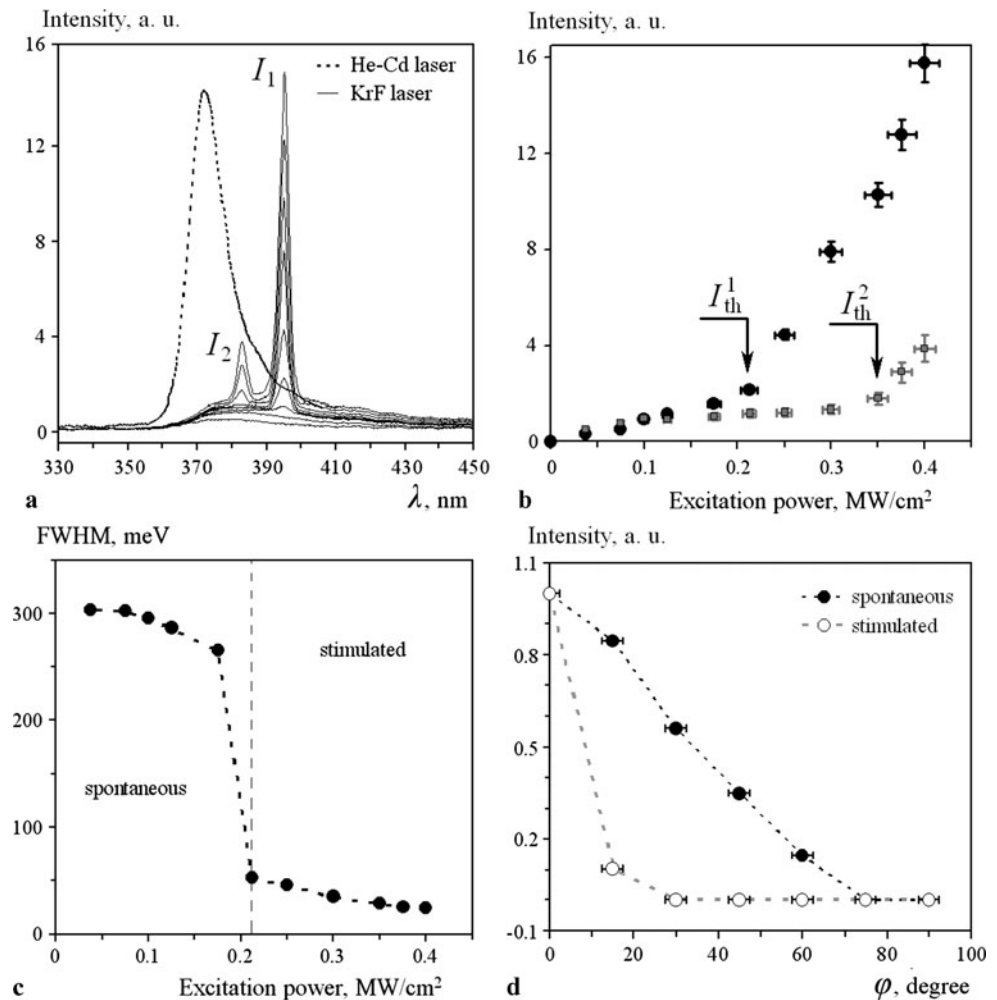
At optical pump power densities up to ~ 210 kW/cm², a wide peak in the PL spectra appeared corresponding to spontaneous emission of excitons inside the quantum well (372 nm). A further increase of pulsed pump power resulted in predominance of a narrow line I_1 near 395.2 nm, shifted to the red spectral region, and the intensity of this line

sharply rises as the excitation power is enhanced (Fig. 7b). The second narrow line I_2 appeared near 383.1 nm at the excitation power of about 330 kW/cm². The line I_1 has been observed earlier in [18], however, the line I_2 is not reported in the literature. The intensity and spectral position of these lasing lines did not change with the temperature in contrast to the spontaneous peak due to excitons inside the quantum well (372 nm).

The full width on a half maximum of MQW $Mg_{0.27}Zn_{0.73}O/ZnO$ emission was changed by the step-wise law at the threshold of excitation power. FWHM of the lasing lines was an order of magnitude lower in comparison with spontaneous emission. An investigation of the PL intensity angle distribution of the 2D structures has shown that stimulated emission is directed and is sharply reduced at a deviation from the normal to the surface unlike spontaneous emission. Figure 7 presents the FWHM (c) and luminescence angle distribution (d) of the lasing I_1 and spontaneous line of the multiple quantum wells $Mg_{0.27}Zn_{0.73}O/ZnO$ with the well width $L_w = 5.2$ nm.

We observed the lasing in the MQW $Mg_{0.27}Zn_{0.73}O/ZnO$ only in the range of $L_w = 3$ –7 nm. The excitation of stimulated emission in the quantum wells was enabled due to the increase of their quantum efficiency. The resonator in the investigated systems could be formed by the top plane of the quantum wells and the bottom plane of the sapphire substrate, which is confirmed by the diagram of PL intensity angle distribution (Fig. 7d). As the difference in refractive indexes ($\Delta n = 0.14$) and the thicknesses of barrier and well layers are small, we did not consider the two-dimensional structures as distributed Bragg reflectors.

Fig. 7 The PL spectra of a MQW $\text{Mg}_{0.27}\text{Zn}_{0.73}\text{O}/\text{ZnO}$ with a well width $L_w = 5.2$ nm: (a) excitation by the He–Cd laser and the excimer KrF laser with pump power up to 400 kW/cm^2 ; (b) dependences of PL intensity of the lines I_1 ($\lambda = 395.2$ nm) and I_2 ($\lambda = 383.1$ nm) of the MQW $\text{Mg}_{0.27}\text{Zn}_{0.73}\text{O}/\text{ZnO}$ on excimer KrF laser pump power. FWHM (c) and luminescence angle distribution (d) of stimulated and spontaneous lines of the MQW $\text{Mg}_{0.27}\text{Zn}_{0.73}\text{O}/\text{ZnO}$ with the well width $L_w = 5.2$ nm



4 Conclusions

The multiple quantum wells $\text{Mg}_{0.27}\text{Zn}_{0.73}\text{O}/\text{ZnO}$ grown by the pulsed laser deposition method have shown high structural quality and sharp interfaces. The interface roughness of the QWs was inherited from the substrate and did not exceed 1 nm. We observed the quantum confinement effect in the two-dimensional heterostructures based on ZnO showing up in a blue shift of exciton energy for the well width reduction. The exciton binding energy of the 2D systems was two times higher in comparison with the bulk ZnO. A sharp increase of the exciton peak intensity in the photoluminescence spectra for a well width reduction is due to an enhancement of quantum efficiency in the MQW $\text{Mg}_{0.27}\text{Zn}_{0.73}\text{O}/\text{ZnO}$ in comparison with the bulk ZnO. We observed that the decreasing of exciton–phonon interaction is caused by the quantum confinement of charge carriers. The effect of stimulated emission excited in the quantum wells by optical pumping appeared at a threshold of $\sim 210 \text{ kW/cm}^2$. The effects mentioned above have a fundamental character, but can be applied in designing light emitting diodes and lasers with a

tunable wavelength and high temperature stability based on the heterostructures $\text{Mg}_x\text{Zn}_{1-x}\text{O}/\text{ZnO}$.

Acknowledgements We gratefully acknowledge the technical and analytical support of Dr. C. Wenzel and Dr. K.D. Shcherbachev. This work was supported by RFBR grants: Nos. 09-08-00291_a, 09-07-00208_a.

References

1. M.J. Bevan, H.D. Shih, J.A. Dodge, A.J. Syllaios, D.F. Weirauch, *J. Electron. Mater.* **27**, 769 (1998)
2. V. Kuryatkov, G. Kipshidze, S.N.G. Chu, M. Holtz, Yu. Kudryavtsev, *Appl. Phys. Lett.* **83**(7) (2003)
3. Y. Ryu, T.-S. Lee, J.A. Lubguban, H.W. White, B.-J. Kim, Y.S. Park, C.J. Youn, *Appl. Phys. Lett.* **88**, 241108 (2006)
4. U. Ozgur, Ya.I. Alivov, C. Liu, A. Teke, M.A. Reshchikov, S. Dogan, V. Avrutin, S.-J. Cho, H.J. Morkoc, *Appl. Phys.* **98**, 041301 (2005)
5. T. Makino, Y. Segava, M. Kawasaki, H. Koinuma, *Semicond. Sci. Technol.* **20** (2005)
6. L.S. Gorbatenko, O.A. Novodvorsky, V.Ya. Panchenko, O.D. Khramova, Ye.A. Cherebilo, A.A. Lotin, C. Wenzel, N. Trumpaicka, J.W. Bartha, *Laser Phys.* **16**, 1152 (2009)

7. A.A. Lotin, O.A. Novodvorsky, E.V. Khaydukov, V.V. Rocheva, O.D. Khramova, V.Ya. Panchenko, C. Wenzel, N. Trumpaicka, K.D. Shcherbachev, *Semiconductors* **44**, 260 (2010)
8. A.A. Lotin, O.A. Novodvorsky, L.S. Parshina, E.V. Khaydukov, O.D. Khramova, V.Ya. Panchenko, *Fizika* **16**, 1 (2010)
9. P.A. Tipler, R.A. Llewellyn, *Modern Physics* (Freeman, New York, 2007)
10. G.-C. Yi, W.I. Park, M.Y. Kim, S.J. Pennycook, *Adv. Mater.* **15**, 526 (2003)
11. W.E. Bowen, W. Wang, E. Cagin, J.D. Phillips, *J. Electron. Mater.* **37**, 749 (2008)
12. J.G. Lu, S. Fujita, T. Kawaharamura, H. Nishinaka, Y. Kamada, T. Ohshima, *Appl. Phys. Lett.* **89**, 262107 (2006)
13. G. Coli, K.K. Bajaj, *Appl. Phys. Lett.* **78**, 2861 (2001)
14. O.L. Lazarenkova, A.N. Pihtin, *Semiconductors* **32**, 1108 (1998)
15. N.B. Brandt, V.A. Kulbachinsky, *Kvazichasticy v fizike kondensirovannogo sostoyaniya*, pp. 367–377 (M.:FIZMATLIT, 2007)
16. E.F. Schubert, *Light-Emitting Diodes* (Cambridge University Press, Troy, 2008)
17. P. Lautenschlager, M. Garriga, S. Logothetidis, M. Cardona, *Phys. Rev. B* **35**, 9174 (1987)
18. T.V. Shubina, A.A. Toropov, O.G. Lublinskaya, P.S. Kop'ev, S.V. Ivanov, A. El-Shaer, M. Al-Suleiman, A. Bakin, A. Waag, A. Voinilovich, E.V. Lutsenko, G.P. Yablonskii, J.P. Bergman, G. Pozina, B. Monemar, *Appl. Phys. Lett.* **91**, 201104 (2007)